Tangential AC Breakdown Strength of Solid-Solid Interfaces Considering Surface Roughness

Emre Kantar, Frank Mauseth, and Erling Ildstad
Department of Electric Power Engineering
Norwegian University of Science and Technology
Trondheim, Norway

Sverre Hvidsten
Electric Power Technology
SINTEF Energy Research
Trondheim, Norway

***Abstract*—Primary purpose of this paper is to study the influence of the surface roughness and interfacial pressure on the tangential AC breakdown strength (BDS) of solid-solid interfaces experimentally. Three-dimensional surface texture parameters are utilized to characterize the morphology of the polymer surfaces. Experiments were performed using samples made of cross-linked polyethylene (XLPE) at three different contact pressures. Surface roughness was varied by polishing the surfaces using four different sandpapers of different roughness. Each surface topography was then assessed using a $3-\mathrm{D}$ optical profilometer. Next, the samples were assembled under ambient laboratory conditions. Experimental results showed a good correlation between the tangential BDS and the surface roughness. The results suggested that reducing the surface roughness resulted in decreased mean height of the surface asperities by nearly 97%. As a result, the tangential BDS rose by a factor of $1.85-2.15$ with increasing pressure. Likewise, increased contact pressure yielded augmented tangential BDS values by a factor of $1.4-1.7$ following the decrease of the roughness.**

I. INTRODUCTION

Although materials and production technologies for power cables, joints and accessories have gained a fair amount of experience over the years, cable connectors and joints are still considered weaker parts of complete cable systems [1], [2]. One of the primary reasons is the presence of solid-solid interfaces [1]–[3]. The combination of two solid dielectrics adversely affects the dielectric performance due to the increased risk of interfacial tracking failure, leading to the formation of a conductive path bridging the electrodes [2]–[4].

One of the main reasons of solid interfaces being weaker than the bulk solid material is caused by the inhomogeneous electric field distribution at the interface since interfaces mostly exist between different materials with different relative permittivity [2], [4]. In Fig. 1(a), a generic cable splice is shown, where Fig. 1(b) reveals the electric field contour lines in two-dimensional profile. As can be seen in Fig. 1(a)−(c), the tangential field component culminates at the polymer interfaces. Besides, prefabricated accessories are generally mated at site in sub-optimal and less controllable conditions, which renders them solid-solid interfaces vulnerable to bad installations [2]. As a consequence, microscopic imperfections (such as cavities, protrusions, and contaminants) occur at the interfaces. Such imperfections reduce the tangential AC electric breakdown strength (BDS) of the interface notably. They are, thus, likely to initiate partial discharges (PD), electrical treeing and a complete flashover might eventually follow [1]–[3], [5].

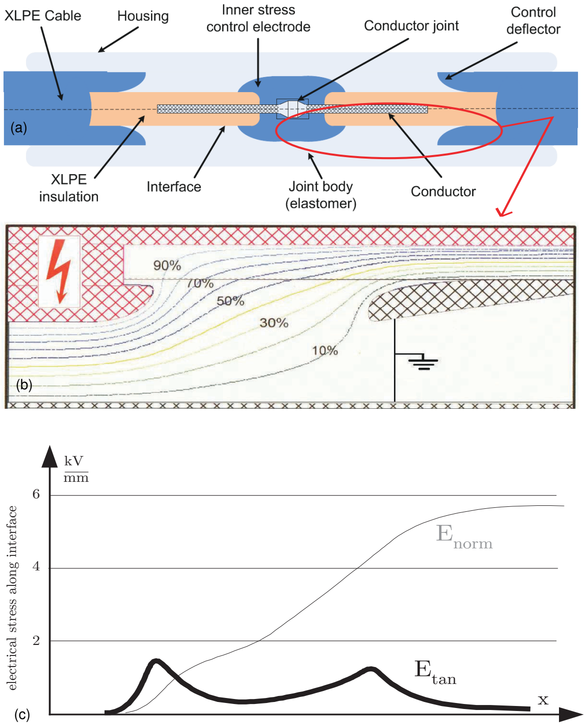

Fig. 1. (a) Prefabricated EHV silicone joint [3]. (b) Field plot [2]. (c) Interface stress [2].

The primary purpose of this paper is to explore the impact of the surface roughness and mechanically applied interfacial pressure on the longitudinal AC breakdown strength of dry-mated polymeric material interfaces experimentally. Areal field parameters are also utilized when differentiating the morphology of the surfaces quantitatively to help interpret the experimental findings. The methodical approach adopted in this work favors the XLPE-XLPE interface since the key purpose is to examine an interface where the materials involved have the same elasticity and can withstand high pressures without any significant deformation over a broad pressure range.

The authors acknowledge the financial support of the Research Council of Norway (project no. 228344) and the SUBCONN Project Consortium.

II. SOLID-SOLID INTERFACES

The assembly of interfaces does not follow an automated process under clean room conditions. When two dielectric surfaces come to contact, plenty of cavities are formed between the tips of the interfacial protrusions. Thus, a cavity-free interfacial surface is not possible to obtain [2]. The cavities on a dielectric surface have various sizes, shapes and distribution. Two most critical cavity types in case of a tangential electric field are the cylindrical cavities in the tangential direction and spherical as illustrated in Fig. 2 [3].

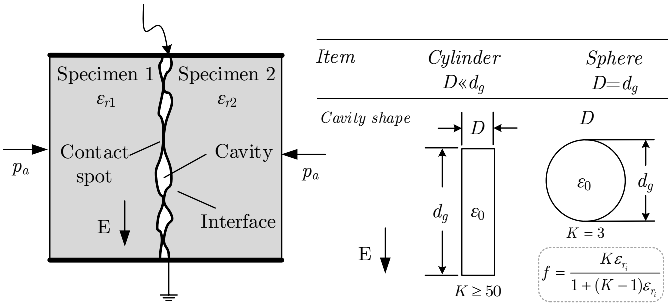

Fig. 2. Air-filled cavities formed on the polymer interface.

When the interface is assembled under dry conditions, the cavities are filled with air. The applied voltage is then distributed along the strings of the cavities and contact spots. The dielectric strength of air is much lower than that of the polymeric insulation, and the field gets intensified in the cavities by the enhancement factor f as shown in Fig. 2. Hence, the dielectric breakdown will first occur in the air-filled cavities, and then the complete flashover presumably takes place immediately [1]. In the case of a homogeneous electric field, the correlation between the cavity size and the breakdown voltage (BDV) thereof is characterized by the Paschen's curve for air [6]. Referring to the left side of the Paschen's curve for air (the left branch of the V$-$shaped curve), Majid et al. [3] addressed that as the cavity length increases, the expected BDV reduces. Considering the findings of Majid et al. [3], we infer that there are a number of air-filled channels traversing the whole interface. Channels are considered a series of cavities linked as a string at the interface in $3-\mathrm{D}$ plane, thus they are vented to the surroundings, and the pressure inside them remains constant at the atmospheric pressure. Besides, the vented channels coexist with numerous interlocked smaller cavities in which the air pressure is likely to increase as a function of the rise in the contact pressure p_a. The BDV of the vented channels is, however, much lower than that of the individual interlocked cavities according to Paschen's law [6]. Thereby, the vented channels are assumed the principal governing mechanism in the interfacial breakdown phenomenon.

Exact length and number of the cavities are unknown and depend heavily on the following parameters: the elasticity of the material, the applied interfacial pressure, and the surface roughness. As illustrated in Fig. 3, in case of the tangentially applied electric field, the increased contact pressure renders the interfacial BDS higher [4]. The reason is that the increased pressure further pushes the tips of the asperities and yields smaller the cavities that in turn augment the interfacial BDS. Likewise, smoother surfaces show as similar an influence on the BDS as the increased pressure, due to the reduced cavity size at the interface. It is worth mentioning that the interfacial BDS is higher than that of air, whereas it is not as strong as the bulk material strength even under a higher contact pressure or a smoother surface [4]. The impact of the surface roughness and the interfacial pressure on the BDS will be interpreted in the discussion using the correlations provided here.

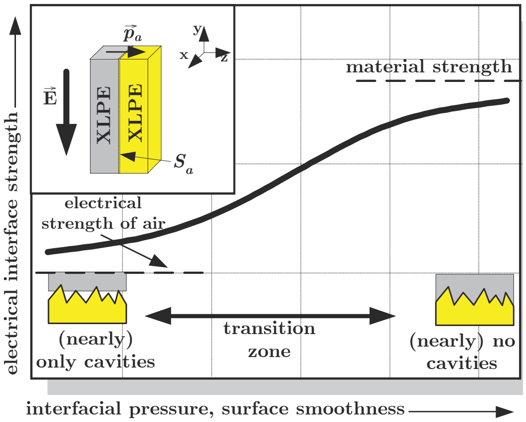

Fig. 3. Tangential breakdown strength of interfaces against interface pressure and the surface roughness/smoothness [4].

III. EXPERIMENTAL PROCEDURE

A. Set-up for AC Breakdown Tests

A simple illustration of the test arrangement with the dimensions of the core components is depicted in Fig. 4(a). There, two rectangular prism-shaped samples ($55\,\mathrm{mm}$ x $25\,\mathrm{mm}$ x $4\,\mathrm{mm}$) were assembled under dry ambient conditions between two Rogowski-type electrodes, forming a $4\,\mathrm{mm}$-wide interface traversed by the tangentially applied field [7].

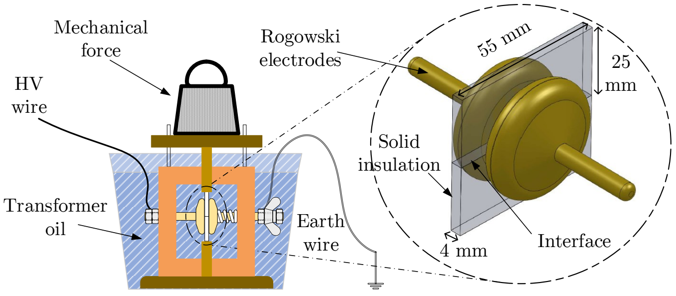

Fig. 4. The simplified sketch of the mechanical test set-up. Electrode diameter $36\,\mathrm{mm}$.

All the breakdown tests were performed with the set-up submerged in an oil-filled container to prevent any external flashover. Also, to avoid oil penetration at the interface, surface pressure was applied before filling the test chamber with the oil. An AC ramp voltage with the rate of $1\,\mathrm{kV/s}$ was applied to the HV wire [7].

B. Polishing the Samples

XLPE samples were cut in the size of $55\,\mathrm{mm}$ x $25\,\mathrm{mm}$ x $4\,\mathrm{mm}$ rectangular prisms from the insulation of a commercially available $145\,\mathrm{kV}$ power cable. The contact surfaces of the samples were prepared using $\mathrm{STRUERS\,Abramin}$ tabletop, rotating grinding machine. Four different sandpapers of different grits (#180, #500, #1000, and #2400) were used. Readers are advised to refer to [7] for further details regarding the preparation and polishing the samples.

C. Examination of Surface Roughness

A 3D optical profilometer $(\mathrm{Bruker\,GT-K})$ was used to obtain the surface topography of the polished XLPE surfaces. The assessment area of the profile was $1.26\,\mathrm{mm}$ x $0.95\,\mathrm{mm}$, which was about 5.5% of the total interfacial area ($4\,\mathrm{mm}$ x $55\,\mathrm{mm}$). Several scans were performed at different sections on each surface to ensure consistency.

The 3D areal surface roughness $S-$height parameters were evaluated according to $\mathrm{ASME\,B46.2-1995}$ standards and are revealed in Fig. 5 in a two-dimensional profile. They are namely: arithmetic mean height/roughness (S_a), minimum profile peak height (S_v), and maximum height of the surface (S_z).

As Leach et al. [8] suggested, the S_a parameter represents an overall measure of the surface texture and can be used to identify the different surfaces under study. Thus, S_a will be used in the first place when a swift comparison is exercised.

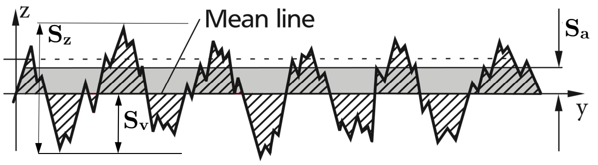

Fig. 5. Schematic representation of the $S-$parameters in a two-dimensional profile [8].

D. Test Procedure & Data Handling

The desired contact pressure was exerted using weights ranging between $11-26\,\mathrm{kg}$ to press the samples against one another vertically. The average contact pressure is then calculated using $p_a = F/A_a$, where F is the exerted force in N and A_a is the interface area in m^2 ($55\,\mathrm{mm}$ x $4\,\mathrm{mm}$).

Eight measurements were performed for each set of experiments by using a virgin pair of samples only once. The obtained results were statistically evaluated using the two-parameter Weibull distribution. For further evaluation, the $63.2\,\mathrm{percentile}$ value with the 90% confidence interval was employed.

IV. RESULTS

A. Surface Characterization

At the roughest surface, the polished surfaces appear to be quite rough with an irregular pattern of cavities formed by high peaks and deep pits/valleys; whereas, it becomes far less irregular with shorter peaks and pits at the smoothest. The obtained roughness $S-$height parameters from the measurements are tabulated in Table I.

TABLE I
SURFACE ROUGHNESS HEIGHT PARAMETERS

Grit No.	Roughness S-parameters		
	S_a [μm]	S_v [μm]	S_z [μm]
#180	8.86	−105.79	181.64
#500	7.79	−60.04	89.18
#1000	1.65	−14.98	36.86
#2400	0.27	−8.76	20.44

B. AC Breakdown Tests

Fig. 6 displays the influence of the surface roughness on the interfacial BDS under 0.5, 0.86 and $1.16\,\mathrm{MPa}$ contact pressures. The errorbars represent the 90% confidence intervals where the markers stand for the $63.2\,\mathrm{percentile}$ values. The $\mathrm{x-}$axis is normalized such that S_a of #2400 is equal to unity.

Only the $63.2\,\mathrm{percentile}$ BDS values are plotted against the sandpaper grit in Fig. 7 to facilitate the interpretation whereas each bar illustrates the arithmetic mean height S_a. The results show that, in all cases, an increased roughness (i.e. higher S_a) results in an reduced BDS, not to mention an increased contact pressure brings about an increased BDS. Besides, the $63.2\,\mathrm{percentile}$ BDS in the case of an interface polished by #2400 is nearly twice as high as that of the interface polished by #180 under each pressure. The rise in the $63.2\,\mathrm{percentile}$ BDS from #180 to #500 and from #180 to #1000 is; however, not as notable, only by a factor of $1.2-1.3$. Finally, Fig. 8 demonstrates the impact of the interfacial pressure on the BDS for each rough surface. Referring to Figs. 7 and 8 and interpreting the effect of the pressure and roughness together, we can infer that the $63.2\,\mathrm{percentile}$ BDS becomes 1.4 times as high for #180 ($S_a = 8.86\,\mu m$). Whereas, it increases by a factor of 1.7 for #2400 ($S_a = 0.27\,\mu\mathrm{m}$) as the pressure is raised from 0.5 to $1.16\,\mathrm{MPa}$.

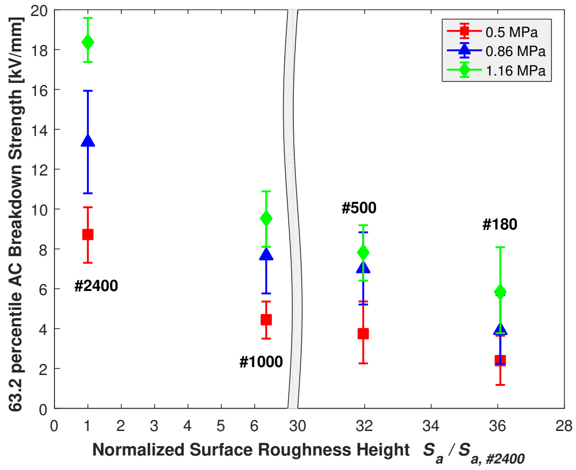

Fig. 6. 63.2 percentile BDS with 90% confidence intervals versus surface roughness represented by the mean roughness height parameter S_a.

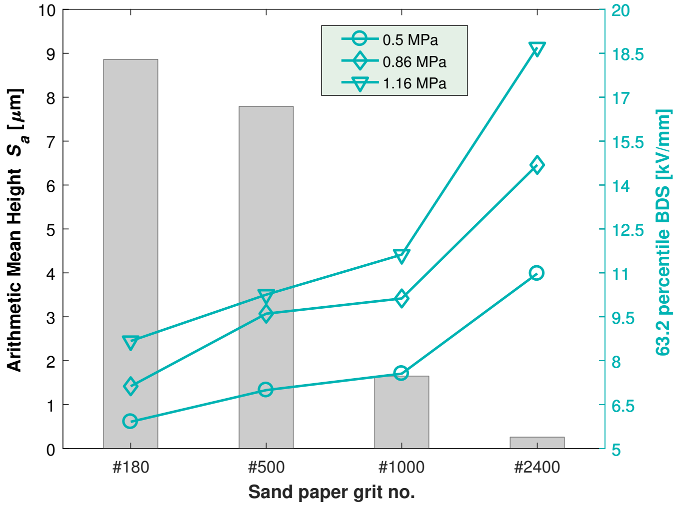

Fig. 7. (i) Left y−axis: Arithmetic mean height S_a shown by bar graphs. (ii) Right y−axis: 63.2 percentile BDS against sandpaper grit.

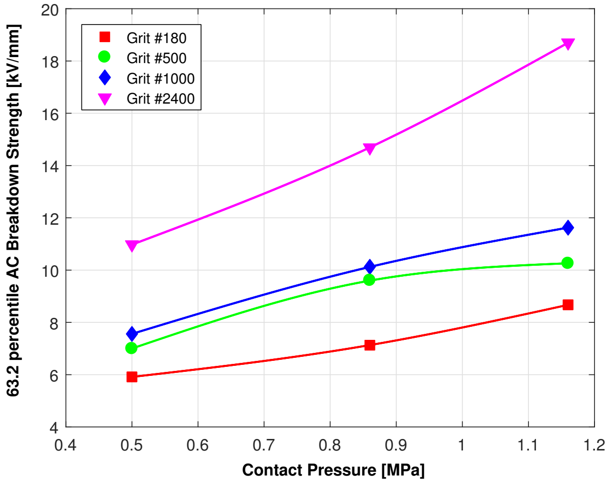

Fig. 8. The 63.2 percentile AC BDS versus contact pressure.

V. DISCUSSION

The rate of change in the 63.2 percentile BDS from #1000 to #2400 culminates under all pressures as evident in Fig. 7, where the highest increase is seen at $1.16\,\mathrm{MPa}$ by a factor of 1.6. Thus, it can be inferred that the smoothness of the surface can play as vital a role as the contact pressure in improving the BDS of the interfaces under dry-mated conditions.

In Fig. 8, as S_a reduces by a factor of 32 from #180 to #2400, the 63.2 percentile BDS increases by 85% at $p_a = 0.5\,\mathrm{MPa}$. Similarly, it rises by 115% at $1.16\,\mathrm{MPa}$. Interpreting the impact of the pressure regarding the correlation introduced in Section II, we deduce that increased interfacial pressure probably reduces the size of the air-filled cavities at the considered surface, where the biggest change in BDS by a factor of 1.7 was observed in the case of the smoothest surface.

Despite the increase in pressure in Fig. 6, the overlap of the errorbars at the same pressure is significant in the case of the roughest surface (#180). Hence, voids of similar size are likely to arise irrespective of the pressure. On the other hand, the overlapping portions of the bars tend to shrink as the surface smoothness increase. In the case of the smoothest surface, no overlap exists in Fig. 6. Greenwood et al. [9] addressed a related finding that the contact area augmented further as the contact pressure was increased, which yielded smaller voids at the interface.

VI. CONCLUSION

The performed roughness measurements and the calculated $S-$height parameters e.g. S_a correlated well with the experimental results. It was observed that the rougher the surface, the higher the peaks and the deeper the valleys in the surface roughness profile, likely to lead to larger cavities at the interface that yield a lower BDS as discovered in the performed tests. It is worth to mention that interfaces could perform as well as the bulk materials when the applied pressure is high enough and the contact surface is as smooth as possible, as observed in the case of #2400 at $1.16\,\mathrm{MPa}$. Thus, the bottom line is interfaces are one of the weakest parts of an electric insulation system. However, it is possible to improve the performance of the polymer interface by introducing a smoother surface and by retaining the interfacial pressure high enough during service life.

REFERENCES

[1] D. Fournier, "Effect of the surface roughness on interfacial breakdown between two dielectric surfaces," in *IEEE Int'l. Sympos. on Electr. Insul.*, vol. 2. IEEE, 1996, pp. 699–702.
[2] D. Kunze, B. Parmigiani, R. Schroth, and E. GocNenbach, "Macroscopic internal interfaces in high voltage cable accessories," in *CIGRE Session*, no. 15–203, 2000.
[3] S. M. Hasheminezhad, "Tangential electric breakdown strength and PD inception voltage of solid-solid interface," Ph.D. dissertation, Norwegian University of Science and Technology, 2016.
[4] J. CIGRE, "21/15: Interfaces in accessories for extruded hv and ehv cables," *Electra*, no. 203, pp. 53–59, 2002.
[5] B. Du, X. Zhu, L. Gu, and H. Liu, "Effect of surface smoothness on tracking mechanism in XLPE-Si-rubber interfaces," *IEEE Trans. Dielectr. Electr. Insul.*, vol. 18, no. 1, pp. 176–181, 2011.
[6] L. A. Dissado and J. C. Fothergill, *Electrical degradation and breakdown in polymers*. IET, 1992, vol. 9.
[7] E. Kantar, S. Hvidsten, F. Mauseth, and E. Ildstad, "On the tangential AC breakdown strength of polymeric interfaces considering elastic modulus," in *IEEE Conf. Electr. Insul. and Dielectr. Phen. (CEIDP)*, unpublished.
[8] R. Leach, *Characterisation of areal surface texture*. Springer, 2013.
[9] J. Greenwood and J. Williamson, "Contact of nominally flat surfaces," in *Proc. the Royal Society of London A: Mathematical, Physical and Engineering Sciences*, vol. 295, no. 1442, 1966, pp. 300–319.